Article

# Synthesis and Characterization of the Homologous M–M Bonded Series Ar‘MMAr‘ (M = Zn, Cd, or Hg; Ar‘ = CH-2,6-(CH-2,6-Pr)) and Related Arylmetal Halides and Hydride Species

Zhongliang Zhu, Marcin Brynda, Robert J. Wright, Roland C. Fischer, W. Alexander Merrill, Eric Rivard, Robert Wolf, James C. Fettinger, Marilyn M. Olmstead, and Philip P. Power

*J. Am. Chem. Soc.*, **2007**, 129 (35), 10847-10857• DOI: 10.1021/ja072682x • Publication Date (Web): 11 August 2007



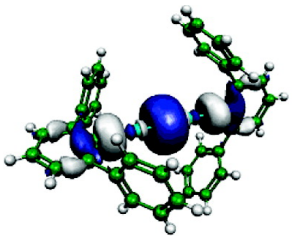

Ar′MMAr′

M = Zn, Cd or Hg

Ar′ = $C_6H_3$-2,6-($C_6H_3$-2,6-$Pr_{i2}$)$_2$

## More About This Article

Additional resources and features associated with this article are available within the HTML version:

- Supporting Information
- Links to the 9 articles that cite this article, as of the time of this article download
- Access to high resolution figures
- Links to articles and content related to this article
- Copyright permission to reproduce figures and/or text from this article

View the Full Text HTML

J|A|C|S
ARTICLES
Published on Web 08/11/2007

# Synthesis and Characterization of the Homologous M−M Bonded Series Ar′MMAr′ (M = Zn, Cd, or Hg; Ar′ = $C_6H_3$-2,6-($C_6H_3$-2,6-$Pr^i_2$)$_2$) and Related Arylmetal Halides and Hydride Species

Zhongliang Zhu, Marcin Brynda, Robert J. Wright, Roland C. Fischer, W. Alexander Merrill, Eric Rivard, Robert Wolf, James C. Fettinger, Marilyn M. Olmstead, and Philip P. Power*

*Contribution from the Department of Chemistry, University of California—Davis, One Shields Avenue, Davis, California 95616*

Received April 17, 2007; E-mail: pppower@ucdavis.edu

***Abstract:*** The synthesis and structural characterization of the first homologous, molecular M−M bonded series for the group 12 metals are reported. The compounds Ar′MMAr′ (M = Zn, Cd, or Hg; Ar′ = $C_6H_3$-2,6-($C_6H_3$-2,6-$Pr^i_2$)$_2$) were synthesized by reduction of the corresponding arylmetal halides by alkali metal/graphite (Zn or Hg) or sodium hydride (Cd). These compounds possess almost linear C−M−M−C core structures with two-coordinate metals. The observed M−M bonds distances were 2.3591(9), 2.6257(5), and 2.5738(3) Å for the zinc, cadmium, and mercury species, respectively. The shorter Hg−Hg bond in comparison to that of Cd−Cd is consistent with DFT calculations which show that the strength of the Hg−Hg bond is greater. The arylmetal halides precursors (Ar′MI)$_{1\text{ or }2}$, and the highly reactive hydrides (Ar′MH)$_{1\text{ or }2}$, were also synthesized and fully characterized by X-ray crystallography (Zn and Cd) and multinuclear NMR spectroscopy. The arylzinc and arylcadmium iodides have iodide-bridged dimeric structures, whereas the arylmercury iodide, Ar′HgI, is monomeric. The arylzinc and arylcadmium hydrides have symmetric (Zn) or unsymmetric (Cd) $\mu$-H-bridged structures. The Ar′HgH species was synthesized and characterized by spectroscopy, but a satisfactory refinement of the structure was precluded by the contamination of monomeric Ar′HgH by Ar′H. It was also shown that the decomposition of Ar′Cd($\mu$-H)$_2$CdAr′ at room temperature leads to the M−M bonded Ar′CdCdAr′, thereby supporting the view that the reduction of the iodide proceeds via the hydride intermediate.

## Introduction

The synthesis of stable molecular compounds featuring homonuclear metal−metal bonds between organo derivatives RMMR (R = organic or related susbstituent) of the group 12 elements (Zn, Cd, and Hg) has proven to be a considerable synthetic challenge. For many years, salt-like, ionic species containing $[Hg_2]^{2+}$ units were the only known group 12 compounds that had been shown to have stable metal−metal bonds.[1] In the 1960s, the work of Corbett and co-workers[2] had shown that the $[Cd_2]^{2+}$ ion existed in aluminum chloride melts, but it was not until 1986 that the structure of a $[Cd_2]^{2+}$ unit in $[Cd_2][AlCl_4]_2$ was reported independently by two different groups.[3] Evidence for the formation of $[Zn_2]^{2+}$ ions was also reported in 1960s within $ZnCl_2$/Zn glasses at high temperatures[4] and later in zeolite matrices.[5] Seemingly, M−M bonding could be stablized only in ionic salts, and molecular M(I) compounds of formula RMMR were thought to exist only as short-lived transient species.[1,6,7] In 1999, Apeloig and co-workers reported the first stable, molecular, $\sigma$-bonded mercury(I) compound in the form of the silyl derivative $Hg_2[Si(SiMe_2SiMe_3)_3]_2$.[8] UV/vis spectroscopy revealed an absorption band at 530 nm that was assigned to a HOMO−LUMO transition involving the Hg−Hg $\sigma$ and $\sigma$* orbitals. Earlier, in 1993, the molecular compound $Cd_2Tp^{Me_2}_2$ ($Tp^{Me_2}$ = hydrotris(3,5-dimethylpyrazolyl)borate) was synthesized by treatment of $CdCl_2$ with $TlTp^{Me_2}$/$LiBHEt_3$ and characterized spectroscopically by Reger and his group.[9] The

(1) Holloway, C. E.; Melník, M. *J. Organomet. Chem.* **1995**, *495*, 1.
(2) (a) Corbett, J. D.; Burkhard, W. J.; Druding, L. F. *J. Am. Chem. Soc.* **1961**, *83*, 76. (b) Corbett, J. D. *Inorg. Chem.* **1962**, *1*, 700. (c) Potts, R. A.; Barnes, R. D.; Corbett, J. D. *Inorg. Chem.* **1968**, *7*, 2558.
(3) (a) Faggiani, R.; Gillespie, R. J.; Vekris, J. E. *J. Chem. Soc., Chem. Commun.* **1986**, 517. (b) Staffel, T.; Meyer, G. *Z. Anorg. Allg. Chem.* **1987**, *548*, 45.
(4) Kerridge, D. H.; Tariq, S. A. *J. Chem. Soc. A* **1967**, 1122.
(5) (a) Rittner, F.; Seidel, A.; Boddenberg, B. *Microporous Mesoporous Mater.* **1998**, *24*, 27. (b) Zhen, S.; Bae, D.; Seff, K. *J. Phys. Chem. B* **2000**, *104*, 515.
(6) (a) Wardell, J. L. In *Comprehensive Organometallic Chemistry*; Wilkinson, G., Stone, F. G. A., Albel, E. W., Eds.; Pergamon, Oxford, 1982; Vol. 2, Chapter 17, p 864. (b) Brodersen, K.; Hummel, H.-U. In *Comprehensive Coordination Chemistry*; Wilkinson, G., Gillard, R. D., McCleverty, J. A., Eds.; Pergamon: Oxford, 1987; Vol. 5, Chapter 56.2, p 1050.
(7) (a) Gade, L. H. *Angew. Chem., Int. Ed.* **1993**, *32*, 24. (b) Schwerdtfeger, P.; Boyd, P. D. W.; Brienne, S.; McFeaters, J. S.; Dolg, M.; Liao, M.-S.; Schwarz, W. H. E. *Inorg. Chim. Acta* **1993**, *213*, 233. (c) Kaupp, M.; von Schnering, H.-G. *Inorg. Chem.* **1994**, *33*, 4179. (d) Liao, M.-S.; Zhang, Q.-E.; Schwarz, W. H. E. *Inorg. Chem.* **1995**, *34*, 5597. (e) Liao, M.-S.; Zhang, Q.-E. *J. Mol. Struct. (Theochem)* **1995**, *358*, 195.
(8) Bravo-Zhivotovskii, D.; Yuzefovich, M.; Bendikov, M.; Klinkhammer, K.; Apeloig, Y. *Angew. Chem., Int. Ed.* **1999**, *38*, 1100.
(9) Reger, D. L.; Mason, S. S.; Rheingold, A. L. *J. Am. Chem. Soc.* **1993**, *115*, 10406.

existence of a Cd−Cd bond in $Cd_2Tp^{Me_2}{}_2$ was established by the observation of $Cd^{111}-Cd^{113}$ coupling in its $^{113}Cd$ NMR spectrum, although an X-ray structure could not be obtained. Later, an example of a molecular zinc hydride with a Zn−Zn bond, $Zn_2H_2$,[10] was trapped in an argon matrix at 12 K and characterized by vibrational spectroscopy, deuterium labeling studies, and theoretical calculations. However, no structurally characterized stable molecule featuring a Zn−Zn bond was synthesized until 2004, when the landmark compound, $Zn_2Cp^*_2$ ($Cp^* = \eta^5$-$C_5Me_5$), was reported by Carmona and co-workers.[11] Subsequent work led to the preparation and characterization of $Zn_2[HC(CMeNAr)_2]_2$ ($Ar = 2,6\text{-}Pr^i_2C_6H_3$)[12] and $Zn_2Ar'_2$ ($Ar' = C_6H_3\text{-}2,6\text{-}(C_6H_3\text{-}2,6\text{-}Pr^i_2)_2$).[13] These results showed that a Zn−Zn bond could be stabilized when suitable ligands were present, and DFT calculations revealed that the nature of the ligands used could have a significant influence on the metal−metal bonding.[11−13] More recently, the first structurally characterized stable molecular species containing a Cd−Cd bond was reported.[14] The currently known metal−metal bonded molecular compounds of group 12 elements display bond distances that increase as the group is descended (Zn < Cd < Hg), as exemplified by the range 2.305(3)−2.3591(9) Å for Zn−Zn bonds,[11−13] 2.6257(5) Å for the Cd−Cd bond in $Cd_2Ar'_2$,[14] and 2.6569(1) Å for the Hg−Hg bond in $Hg_2[Si(SiMe_2SiMe_3)_3]_2$.[8] However, theoretical calculations including relativistic and correlation effects, as well as the influence of the lanthanide contraction, consistently predict that the covalent radius of mercury should be smaller than that of cadmium.[7,15] A similar contraction trend is also present in neighboring group 11 compounds, which is confirmed by both theoretical calculations and structural data.[16] We were therefore eager to synthesize the first complete, homologous series of group 12 metal−metal bonded molecular compounds in order to test the theoretical prediction. In addition, we thought it desirable to synthesize the closely related metal hydride derivatives for two reasons: First, the characterization of such hydrides would allow experimental comparison of the metal−metal separations in the metal−metal bonded and metal hydride compounds.[17] Second, well-characterized group 12 molecular metal hydrides are relatively scarce,[9,13,18−20] and the use of the bulky terphenyl ligands for their stabilization would afford an opportunity to study their properties.

We now describe the synthesis and characterization of a series of molecular group 12 compounds, $M_2Ar'_2$ (M = Zn, Cd, or Hg), as well as the corresponding hydrides $(Ar'MH)_{1\text{ or }2}$, and discuss their structures and bonding in detail.

## Experimental Section

**General Procedures.** All manipulations were carried out by using modified Schlenk techniques under an atmosphere of $N_2$ or in a Vacuum Atmospheres HE-43 drybox. Solvents were dried according to the method of Grubbs[21] and degassed prior to use. The chemicals used in this study were purchased from Aldrich or Acros and used as received. The lithium aryl, LiAr′, was prepared as previously described.[22] $^1H$, $^{13}C$, $^{113}Cd$, and $^{199}Hg$ NMR spectra were recorded on Varian 300 and 600 MHz spectrometers. The $^{113}Cd$ NMR spectra were referenced externally to 0.01 M $Cd(ClO_4)_2$, while the $^{199}Hg$ NMR spectra were referenced externally to a neat sample of $HgMe_2$. (***Caution:*** *Cadmium and mercury compounds are well known for their toxicity. $HgMe_2$ is a highly dangerous neurotoxin that requires great care in its handling. Ingestion or skin contact must be rigorously avoided.*) Infrared data were recorded as Nujol mulls using a Perkin-Elmer 1430 instrument. Melting points were recorded in sealed capillaries using a Meltemp apparatus and are uncorrected.

**Ar′Zn(μ-I)$_2$ZnAr′ (1).** Ar′Li (2.00 g, 4.95 mmol) and $ZnI_2$ (1.59 g, 4.95 mmol) were combined with diethyl ether (50 mL) and stirred for 2 d. The solvent was then removed under a dynamic vacuum, and the residue was extracted with toluene (50 mL). The resultant slurry was allowed to settle, and the mother liquor was separated from the precipitate (LiI) by filtration. The toluene was removed from the filtrate, and the residue was washed with *ca.* 10 mL of cold hexane. The isolated colorless powder was redissolved in warm toluene (*ca.* 20 mL), followed by overnight cooling to *ca.* −18 °C, which afforded X-ray-quality crystals of **1**. Yield: 1.82 g, 62%; mp >360 °C. $^1H$ NMR (300 MHz, $C_6D_6$, 25 °C): $\delta$ 1.08 (d, 12H, *o*-CH(C$H_3$)$_2$, $^3J_{HH} = 6.9$ Hz), 1.23 (d, 12H, *o*-CH(C$H_3$)$_2$, $^3J_{HH} = 6.9$ Hz), 3.00 (sept, 4H, C$H$(CH$_3$)$_2$, $^3J_{HH} = 6.9$ Hz), 7.15−7.34 (m, 9H, *m*-$C_6H_3$, *p*-$C_6H_3$, *m*-Dipp, and *p*-Dipp (Dipp = $C_6H_3$-2,6-$Pr^i_2$)). $^{13}C\{^1H\}$ NMR ($C_6D_6$, 100.6 MHz, 25 °C): $\delta$ 24.2 (CH(*C*H$_3$)$_2$), 25.4 (CH(*C*H$_3$)$_2$), 30.5 (*C*H(CH$_3$)$_2$), 123.6 (*m*-Dipp), 127.1 (*p*-$C_6H_3$), 127.9 (*p*-Dipp), 128.7 (*m*-$C_6H_3$), 142.8 (*i*-Dipp), 146.8 (*o*-$C_6H_3$), 148.0 (*o*-Dipp), 153.4 (*i*-$C_6H_3$).

**Ar′Cd(μ-I)$_2$CdAr′ (2).** Compound **2** was prepared in a way similar to that described for **1**, starting from Ar′Li (1.11 g, 2.73 mmol) and $CdI_2$ (1.00 g, 2.73 mmol). After the reaction mixture was stirred for 2 d, hexane (50 mL) was used to extract the crude compound. The hexane was removed, and the pale yellow residue was extracted again with hexane (50 mL). The solution was then filtered, and the volume was concentrated to *ca.* 10 mL. Storage of the hexane solution for 4 d in a


(10) (a) Greene, T. M.; Brown, W.; Andrews, L.; Downs, A. J.; Chertihin, G. V.; Runeberg, N.; Pyykkö, P. *J. Phys. Chem.* **1995**, *99*, 7925. (b) Wang, X.; Andrews, L. *J. Phys. Chem. A* **2004**, *108*, 11006.

(11) (a) Resa, I.; Carmona, E.; Gutiérrez-Puebla, E.; Monge, A. *Science* **2004**, *305*, 1136. (b) del Río, D.; Galindo, A.; Resa, I.; Carmona, E. *Angew. Chem., Int. Ed.* **2005**, *44*, 1244. (c) Grirrane, A.; Resa, I.; Rodríguez, A.; Carmona, E.; Alvarez, E.; Gutiérrez-Puebla, E.; Monge, A.; Galindo, A.; del Río, D.; Andersen, R. A. *J. Am. Chem. Soc.* **2007**, *129*, 693.

(12) Wang, Y.; Quillian, B.; Wei, P.; Wang, H.; Yang, X.-J.; Xie, Y.; King, R. B.; Schleyer, P. v. R.; Schaefer, H. F.; Robinson, G. H. *J. Am. Chem. Soc.* **2005**, *127*, 11944.

(13) Zhu, Z.; Wright, R. J.; Olmstead, M. M.; Rivard, E.; Brynda, M.; Power, P. P. *Angew. Chem., Int. Ed.* **2006**, *45*, 5807.

(14) Zhu, Z.; Fischer, R. C.; Fettinger, J. C.; Rivard, E.; Brynda, M.; Power, P. P. *J. Am. Chem. Soc.* **2006**, *128*, 15068.

(15) (a) Desclaux, J. P. *At. Data Nucl. Data Tables* **1973**, *i2*, 311. (b) Ziegler, T.; Snijders, J. G.; Baerends, E. J. *J. Chem. Phys.* **1981**, *74*, 1271. (c) Pyykkö, P. *Chem. Rev.* **1988**, *88*, 563.

(16) (a) Schwerdtfeger, P.; Dolg, M.; Schwarz, W. H. E.; Bowmaker, G. A.; Boyd, P. D. W. *J. Chem. Phys.* **1989**, *91*, 1762. (b) Schwerdtfeger, P.; Boyd, P. D. W.; Burrell, A. K.; Robinson, W. T.; Taylor, M. J. *Inorg. Chem.* **1990**, *29*, 3593. (c) Bayler, A.; Schier, A.; Bowmaker, G. A.; Schmidbaur, H. *J. Am. Chem. Soc.* **1996**, *118*, 7006.

(17) It is often experimentally difficult to disprove the presence of a bridging hydride ligand by X-ray crystallography. For further aspects of this problem, see the following: (a) Schneider, J. J.; Goddard, R.; Werner, S.; Krüger, C. *Angew. Chem., Int. Ed.* **1991**, *30*, 1124. (b) Abrahamson, H. B.; Niccolai, G. P.; Heinekey, D. M.; Casey, C. P.; Bursten, B. *Angew. Chem., Int. Ed.* **1992**, *31*, 471. (c) Kersten, J. L.; Rheingold, A. L.; Theopold, K. H.; Casey, C. P.; Widenhoefer, R. A.; Hop, C. E. C. A. *Angew. Chem., Int. Ed.* **1992**, *31*, 1341. (d) Lutz, F.; Bau, R.; Wu, P.; Koetzle, T. F.; Krüger, C.; Schneider, J. J. *Inorg. Chem.* **1996**, *35*, 2698.

(18) Some organozinc hydride examples: (a) Bell, N. A.; Moseley, P. T.; Shearer, H. M. M.; Spencer, C. B. *J. Chem. Soc., Chem. Commun.* **1980**, 359. (b) Looney, A.; Han, R.; Gorrell, I. B.; Cornebise, M.; Yoon, K.; Parkin, G.; Rheingold, A. L. *Organometallics* **1995**, *14*, 274. (c) Kläui, W.; Schilde, U.; Schmidt, M. *Inorg. Chem.* **1997**, *36*, 1598. (d) Krieger, M.; Neumüller, B.; Dehnicke, K. *Z. Anorg. Allg. Chem.* **1998**, *624*, 1563. (e) Hao, H. J.; Cui, C. M.; Roesky, H. W.; Bai, G. C.; Schmidt, H.-G.; Noltemeyer, M. *Chem. Commun.* **2001**, 1118.

(19) Some molecular cadmium hydride complexes: (a) Kimblin, C.; Bridgewater, B. M.; Churchill, D. G.; Hascall, T.; Parkin, G. *Inorg. Chem.* **2000**, *39*, 4240. (b) Dowling, C. M.; Parkin, G. *Polyhedron* **2001**, *20*, 285. (c) Philson, L. A.; Alyounes, D. M.; Zakharov, L. N.; Rheingold, A. L.; Rabinovich, D. *Polyhedron* **2003**, *22*, 3461.

(20) Some spectroscopically characterized organomercury hydrides: (a) Devaud, M. *J. Organomet. Chem.* **1981**, *220*, C27. (b) Bellec, N.; Guillemin, J.-C. *Tetrahedron Lett.* **1995**, *36*, 6883. (c) Greene, T. M.; Andrews, L.; Downs, A. J. *J. Am. Chem. Soc.* **1995**, *117*, 8180. (d) Nakamura, E.; Yu, Y.; Mori, S.; Yamago, S. *Angew. Chem., Int. Ed.* **1997**, *36*, 374.

(21) Pangborn, A. B.; Giardello, M. A.; Grubbs, R. H.; Rosen, R. K.; Timmers, F. J. *Organometallics* **1996**, *15*, 1518.

(22) Schiemenz, B.; Power, P. P. *Angew. Chem., Int. Ed.* **1996**, *35*, 2150.

freezer (*ca.* −50 °C) afforded colorless, X-ray-quality crystals of **2**. Yield: 1.17 g, 67%; mp 287 °C. $^1$H NMR (300 MHz, $C_6D_6$, 25 °C): $\delta$ 1.07 (d, 12H, CH(C$H_3$)$_2$, $^3J_{HH}$ = 6.6 Hz), 1.24 (d, 12H, CH(C$H_3$)$_2$, $^3J_{HH}$ = 6.9 Hz), 2.99 (sept, 4H, C$H$(CH$_3$)$_2$, $^3J_{HH}$ = 7.2 Hz), 7.13−7.31 (m, 9H, *m*-$C_6H_3$, *p*-$C_6H_3$, *m*-Dipp, and *p*-Dipp). $^{13}$C{$^1$H} NMR ($C_6D_6$, 100.6 MHz, 25 °C): $\delta$ 24.5 (CH(*C*H$_3$)$_2$), 25.2 (CH(*C*H$_3$)$_2$), 30.6 (*C*H(CH$_3$)$_2$), 123.7 (*m*-Dipp), 126.7 (*p*-$C_6H_3$), 127.8 (*p*-Dipp), 128.9 (*m*-$C_6H_3$), 144.2 (*i*-Dipp), 146.6 (*o*-$C_6H_3$), 148.2 (*o*-Dipp), 162.3 (*i*-$C_6H_3$). $^{113}$Cd{$^1$H} ($C_6D_6$, 133.1 MHz, 25 °C): $\delta$ 210.9.

**Ar′HgI (3).** *Method A:* Compound **3** was prepared in a way similar to that described for **1** from Ar′Li (4.00 g, 9.89 mmol) and $HgI_2$ (4.49 g, 9.89 mmol). After the reaction mixture was stirred for 2 d, toluene (150 mL) was used to extract the crude compound. Upon removal of the toluene, a white fine powder was obtained. *Method B*: Compound **3** can also be obtained by the treatment of Ar′MgBr·2THF (**11**, 4.00 g, 6.19 mmol) with $HgI_2$ (2.81 g, 6.19 mmol), followed by the same workup as that of Method A. Storage of the resulting product in hexane (*ca.* 0.2 g in 10 mL) for 1 d at *ca.* −18 °C afforded colorless, X-ray-quality crystals of **3**. Yield: 4.32 g, 60% (Method A) and 4.14 g, 91.9% (Method B); mp 223 °C. $^1$H NMR (300 MHz, $C_6D_6$, 25 °C): $\delta$ 1.07 (d, 12H, CH(C$H_3$)$_2$, $^3J_{HH}$ = 6.6 Hz), 1.24 (d, 12H, CH(C$H_3$)$_2$, $^3J_{HH}$ = 6.9 Hz), 2.99 (sept, 4H, C$H$(CH$_3$)$_2$, $^3J_{HH}$ = 7.2 Hz), 7.13−7.31 (m, 9H, *m*-$C_6H_3$, *p*-$C_6H_3$, *m*-Dipp, and *p*-Dipp). $^{13}$C{$^1$H} NMR ($C_6D_6$, 100.6 MHz, 25 °C): $\delta$ 24.5 (CH(*C*H$_3$)$_2$), 25.2 (CH(C*H*$_3$)$_2$), 30.6 (*C*H(CH$_3$)$_2$), 123.7 (*m*-Dipp), 126.7 (*p*-$C_6H_3$), 127.8 (*p*-Dipp), 128.9 (*m*-$C_6H_3$), 144.2 (*i*-Dipp), 146.6 (*o*-$C_6H_3$), 148.2 (*o*-Dipp), 162.3 (*i*-$C_6H_3$). $^{199}$Hg{$^1$H} NMR ($C_6D_6$, 107.4 MHz, 25 °C): $\delta$ −1293.6.

**Zn$_2$Ar′$_2$ (4).** A solution of **1** (0.93 g, 1.58 mmol) in diethyl ether (50 mL) was added to a Schlenk tube containing finely cut sodium (0.036 g, 1.58 mmol) at ambient temperature. After the reaction mixture was stirred for 2 d, some Zn metal had precipitated. The solution was then filtered, and the solvent was removed under a dynamic vacuum. The residue was redissolved in hexane (5 mL), and storage for 2 d in a freezer (*ca.* −40 °C) afforded large, colorless, X-ray-quality crystals of **4**. Yield: 0.174 g, 24%; mp >360 °C (when the temperature was kept near 360 °C for 5 min, **4** decomposed and a black solid was deposited). $^1$H NMR (300 MHz, $C_6D_6$, 25 °C): $\delta$ 1.00 (d, 12H, *o*-CH(C$H_3$)$_2$, $^3J_{HH}$ = 6.9 Hz), 1.12 (d, 12H, *o*-CH(C$H_3$)$_2$, $^3J_{HH}$ = 6.9 Hz), 2.86 (sept, 4H, C$H$(CH$_3$)$_2$, $^3J_{HH}$ = 6.9 Hz), 7.06−7.24 (m, 9H, *m*-$C_6H_3$, *p*-$C_6H_3$, *m*-Dipp, and *p*-Dipp). $^{13}$C{$^1$H} NMR ($C_6D_6$, 100.6 MHz, 25 °C): $\delta$ 24.7 (CH(*C*H$_3$)$_2$), 24.8 (CH(*C*H$_3$)$_2$), 30.4 (*C*H(CH$_3$)$_2$), 123.0 (*m*-Dipp), 125.7 (*p*-$C_6H_3$), 127.6 (*p*-Dipp), 128.3 (*m*-$C_6H_3$), 142.3 (*i*-Dipp), 146.9 (*o*-$C_6H_3$), 147.4 (*o*-Dipp), 162.4 (*i*-$C_6H_3$).

**Cd$_2$Ar′$_2$ (5).** The iodide derivative **2** (1.00 g, 1.57 mmol) and NaH (0.075 g, 3.14 mmol) were combined with THF (50 mL) and stirred for 3 d. The solvent was then removed under a dynamic vacuum, and the residue was extracted with benzene (50 mL). The slurry was allowed to settle, and the mother liquor was decanted from the precipitate (NaI and excess NaH). The volume was concentrated to *ca.* 10 mL, and storage for 2 d in a refrigerator (*ca.* 8 °C) afforded colorless, X-ray-quality crystals of **5**. Yield: 0.22 g, 28% (based on **2**); decomposition of **5** to a gel-like gray solid was seen at 182 °C. $^1$H NMR (300 MHz, $C_6D_6$, 25 °C): $\delta$ 1.05 (d, 12H, CH(C$H_3$)$_2$, $^3J_{HH}$ = 7.2 Hz), 1.12 (d, 12H, CH(C$H_3$)$_2$, $^3J_{HH}$ = 6.6 Hz), 2.95 (sept, 4H, C$H$(CH$_3$)$_2$, $^3J_{HH}$ = 6.9 Hz), 7.10−7.27 (m, 9H, *m*-$C_6H_3$, *p*-$C_6H_3$, *m*-Dipp, and *p*-Dipp). $^{13}$C{$^1$H} NMR ($C_6D_6$, 100.6 MHz, 25 °C): $\delta$ 24.3 (CH(*C*H$_3$)$_2$), 24.9 (CH(*C*H$_3$)$_2$), 30.4 (*C*H(CH$_3$)$_2$), 122.9 (*m*-Dipp), 125.8 (*p*-$C_6H_3$), 127.1 (*p*-Dipp), 128.6 (*m*-$C_6H_3$), 144.0 (*i*-Dipp), 147.0 (*o*-$C_6H_3$), 147.2 (*o*-Dipp), 176.5 (*i*-$C_6H_3$). $^{113}$Cd{$^1$H} NMR ($C_6D_6$, 133.1 MHz, 25 °C): $\delta$ 540.3 ($^1J_{CdCd}$ = 8650 Hz).

**Hg$_2$Ar′$_2$ (6).** With rapid stirring, a solution of the iodide derivative **3** (2.00 g, 2.76 mmol) in 50 mL of diethyl ether was added dropwise to freshly prepared $KC_8$ (0.37 g, 2.76 mmol) with cooling in an ice bath. The resulting dark suspension was stirred for 36 h to ensure complete reduction. The solvent was removed, and the residue was extracted with benzene (50 mL) and filtered. Upon removal of the benzene, a white fine powder was obtained. Dissolving a sample of **6** in $C_6D_6$, followed by cooling for 2 d (*ca.* 8 °C), afforded colorless, X-ray-quality crystals. Yield: 0.60 g, 18%; mp >360 °C. $^1$H NMR (300 MHz, $C_6D_6$, 25 °C): $\delta$ 1.05 (d, 12H, CH(C$H_3$)$_2$, $^3J_{HH}$ = 6.6 Hz), 1.12 (d, 12H, CH(C$H_3$)$_2$, $^3J_{HH}$ = 6.6 Hz), 2.89 (sept, 4H, C$H$(CH$_3$)$_2$, $^3J_{HH}$ = 7.2 Hz), 7.10−7.31 (m, 9H, *m*-$C_6H_3$, *p*-$C_6H_3$, *m*-Dipp, and *p*-Dipp). $^{13}$C{$^1$H} NMR ($C_6D_6$, 100.6 MHz, 25 °C): $\delta$ 24.0 (CH(*C*H$_3$)$_2$), 24.9 (CH(*C*H$_3$)$_2$), 30.4 (*C*H(CH$_3$)$_2$), 122.8 (*m*-Dipp), 127.1 (*p*-$C_6H_3$), 127.9 (*p*-Dipp), 128.3 (*m*-$C_6H_3$), 141.8 (*i*-Dipp), 146.2 (*o*-$C_6H_3$), 147.1 (*o*-Dipp), 200.0 (*i*-$C_6H_3$). $^{199}$Hg{$^1$H} NMR ($C_6D_6$, 107.4 MHz, 25 °C): $\delta$ 150.5.

**Ar′Zn($\mu$-H)$_2$ZnAr′ (7).** The iodide derivative **1** (1.00 g, 1.70 mmol) and NaH (0.060 g, 2.50 mmol) were combined with THF (50 mL) at ambient temperature. After the reaction mixture was stirred for 2 d, the solvent was removed, and the residue was extracted with *ca.* 50 mL of hexane. The slurry was allowed to settle, and the mother liquor was separated from the precipitate (NaI and excess NaH). The volume was concentrated to *ca.*10 mL, and storage for 2 d in a freezer (*ca.* −40 °C) afforded colorless, X-ray-quality crystals of **7**. Yield: 0.81 g, 89% (based on **1**); mp 234 °C (loss of crystallinity began at 210 °C, and decomposition of **7** to a black solid was seen at 290 °C). $^1$H NMR (300 MHz, $C_6D_6$, 25 °C): $\delta$ 1.01 (d, 12H, *o*-CH(C$H_3$)$_2$, $^3J_{HH}$ = 6.9 Hz), 1.11 (d, 12H, *o*-CH(C$H_3$)$_2$, $^3J_{HH}$ = 6.9 Hz), 2.91 (sept, 4H, C$H$(CH$_3$)$_2$, $^3J_{HH}$ = 6.9 Hz), 4.84 (s, 1H, Zn*H*), 7.04−7.25 (m, 9H, *m*-$C_6H_3$, *p*-$C_6H_3$, *m*-Dipp, and *p*-Dipp). $^{13}$C{$^1$H} NMR ($C_6D_6$, 100.6 MHz, 25 °C): $\delta$ 24.3 (CH(*C*H$_3$)$_2$), 25.1 (CH(*C*H$_3$)$_2$), 30.6 (*C*H(CH$_3$)$_2$), 123.2 (*m*-Dipp), 126.0 (*p*-$C_6H_3$), 127.8 (*p*-Dipp), 128.5 (*m*-$C_6H_3$), 143.4 (*i*-Dipp), 146.7 (*o*-$C_6H_3$), 148.7 (*o*-Dipp), 155.7 (*i*-$C_6H_3$). IR (Nujol): $\nu_{(Zn-H)}$ bands were not observed and may be very weak or obscured by overlapping ligand absorptions.

**Ar′Zn($\mu$-H)($\mu$-Na)ZnAr′ (8).** Compound **1** (0.50 g, 1.08 mmol) and NaH (0.039 g, 1.62 mmol) were combined in THF (50 mL) in a Schlenk tube. The mixture was stirred for 2 d, the solvent was then removed under a dynamic vacuum, and the residue was extracted with toluene (50 mL). The slurry was allowed to settle, and the mother liquor was separated from the precipitate (NaH) using a filter cannula. The solvent volume was concentrated to *ca.* 10 mL, and storage of product for 2 d in a freezer (*ca.* −18 °C) afforded colorless, X-ray-quality crystals of **8**. Yield: 1.03 g, 87% (based on **7**); decomposed before melting (gas evolution at 235 °C, and at *ca.* 268 °C it became a black solid). Yield: 0.40 g, 87% (based on **1**). $^1$H NMR (300 MHz, $C_6D_6$, 25 °C): $\delta$ 1.09 (d, 12H, *o*-CH(C$H_3$)$_2$, $^3J_{HH}$ = 6.9 Hz), 1.15 (d, 12H, *o*-CH(C$H_3$)$_2$, $^3J_{HH}$ = 6.9 Hz), 2.04 (broad peak, 1H, (Ar′Zn)$_2$·Na*H*), 2.99 (sept, 4H, C$H$(CH$_3$)$_2$, $^3J_{HH}$ = 6.6 Hz), 7.01−7.27 (m, 9H, *m*-$C_6H_3$, *p*-$C_6H_3$, *m*-Dipp, and *p*-Dipp). $^{13}$C{$^1$H} NMR ($C_6D_6$, 100.6 MHz, 25 °C): $\delta$ 23.6 (CH(*C*H$_3$)$_2$), 25.2 (CH(*C*H$_3$)$_2$), 30.7 (*C*H(CH$_3$)$_2$), 122.4 (*m*-Dipp), 127.3 (*p*-$C_6H_3$), 146.8 (*i*-Dipp), 148.1 (*o*-$C_6H_3$), 148.8 (*o*-Dipp), 158.7 (*i*-$C_6H_3$); *m*-$C_6H_3$ and *p*-Dipp resonances are likely obscured by the $C_6H_6$ signal. IR (Nujol): $\nu_{(Zn-H)}$ bands obscured by overlapping ligand absorptions.

**Ar′Cd($\mu$-H)$_2$CdAr′ (9).** Compound **9** was prepared in a way similar to that described for **7** from the iodide derivative **2** (1.00 g, 1.57 mmol) and NaH (0.045 g, 1.89 mmol). The product was obtained as colorless, X-ray-quality crystals. Yield: 0.71 g, 88%; compound **9** is temperature sensitive and at room temperature it partially decomposes into **5** in a few hours. $^1$H NMR (300 MHz, $C_6D_6$, 25 °C): $\delta$ 1.11 (d, 12H, *o*-CH(C$H_3$)$_2$, $^3J_{HH}$ = 6.6 Hz), 1.20 (d, 12H, *o*-CH(C$H_3$)$_2$, $^3J_{HH}$ = 6.9 Hz), 3.07 (sept, 4H, C$H$(CH$_3$)$_2$, $^3J_{HH}$ = 7.2 Hz), 6.84 (s, 1H, Cd*H*), 7.14−7.28 (m, 9H, *m*-$C_6H_3$, *p*-$C_6H_3$, *m*-Dipp, and *p*-Dipp). $^{13}$C{$^1$H} NMR ($C_6D_6$, 100.6 MHz, 25 °C): $\delta$ 24.3 (CH(*C*H$_3$)$_2$), 24.8 (CH(*C*H$_3$)$_2$), 30.5 (*C*H(CH$_3$)$_2$), 123.5 (*m*-Dipp), 126.2 (*p*-$C_6H_3$), 127.9 (*p*-Dipp), 128.6 (*m*-$C_6H_3$), 144.3 (*i*-Dipp), 147.0 (*o*-$C_6H_3$), 148.3 (*o*-Dipp), 166.4 (*i*-$C_6H_3$). $^{113}$Cd{$^1$H} NMR ($C_7D_8$, 133.1 MHz, −40 °C): $\delta$ 410.7 (broad peak). IR (Nujol): $\nu_{(Cd-H)}$ bands obscured by overlapping ligand absorptions.

**Ar′HgH (10).** Compound **10** was prepared in a way similar to that described for **7** starting from the iodide derivative **3** (1.00 g, 1.57 mmol) and KH (0.075 g, 1.88 mmol). A colorless solid mixture of **10** and Ar′H was obtained after workup. Yield: 0.25 g, 31% (based on **3**, yield determined by $^1$H NMR). $^1$H NMR (600 MHz, $C_6D_6$, 25 °C): $\delta$ 1.10 (d, 12H, CH(C$H_3$)$_2$, $^3J_{HH}$ = 6.6 Hz), 1.20 (d, 12H, CH(C$H_3$)$_2$, $^3J_{HH}$ = 6.6 Hz), 3.01 (sept, 4H, C$H$(CH$_3$)$_2$, $^3J_{HH}$ = 7.2 Hz), 7.15−7.32 (m, 9H, *m*-C$_6$H$_3$, *p*-C$_6$H$_3$, *m*-Dipp, and *p*-Dipp), 14.59 (s, 1H, Hg$H$, $^1J_{HgH}$ = 2900 Hz). $^{13}$C{$^1$H} NMR ($C_6D_6$, 100.6 MHz, 25 °C): $\delta$ 24.1 (CH(C$H_3$)$_2$), 24.8 (CH(C$H_3$)$_2$), 30.6 (C$H$(CH$_3$)$_2$), 123.2 (*m*-Dipp), 128.7 (*m*-C$_6$H$_3$), 141.8 (*i*-Dipp), 147.2 (*o*-C$_6$H$_3$), 147.5 (*o*-Dipp), 179.7 (*i*-C$_6$H$_3$); *p*-C$_6$H$_3$ and *p*-Dipp resonances are likely obscured by the $C_6H_6$ signal. $^{199}$Hg{$^1$H} NMR ($C_6D_6$, 107.4 MHz, 25 °C): $\delta$ −659.0 (d, $^1J_{HgH}$ = 2910 Hz).

**Ar′MgBr·2THF (11).** Compound **11** was prepared by a modification of the procedure described for Ar′I.[23] A solution of 560 mmol of DippMgBr (Dipp = C$_6$H$_3$-2,6-Pr$^i_2$) in THF (750 mL) was added dropwise to a stirred solution of 1,3-dichlorobenzene (36.74 g, 250 mmol) in THF (1300 mL) with previously added *n*-BuLi (100 mL of 2.5 M solution in hexanes) in an dry ice/acetone bath. Stirring was continued overnight with slow warming to ambient temperature, after which time the mixture was heated to reflux for 2 h. The solvent was then removed *in vacuo*, and the residue was washed with hexanes (300 mL) and extracted with warm toluene (500 mL). The resultant slurry was allowed to settle, and the mother liquor was separated from the precipitate ($Mg_2$ and Li) salts by filtration. The volume was concentrated to *ca.* 400 mL, and storage for 2 d in a refrigerator (8 °C) afforded colorless crystals of **11**, which were further washed with a small amount of cold hexane (50 mL). Second and third crops of **11** were obtained by continued concentration and cooling of the mother liquor. Yield: 71.3 g, 44% (combined yield); mp 175 °C. $^1$H NMR (300 MHz, $C_6D_6$, 25 °C): $\delta$ 1.16 (d, 12H, CH(C$H_3$)$_2$, $^3J_{HH}$ = 6.6 Hz), 1.17 (s br, 8H, (C$H_2$CH$_2$)$_2$O), 1.39 (d, 12H, CH(C$H_3$)$_2$, $^3J_{HH}$ = 6.6 Hz), 3.24 (s br, 8H, (CH$_2$C$H_2$)$_2$O), 3.42 (sept, 4H, C$H$(CH$_3$)$_2$, $^3J_{HH}$ = 6.6 Hz), 7.15−7.33 (m, 9H, *m*-C$_6$H$_3$, *p*-C$_6$H$_3$, *m*-Dipp, and *p*-Dipp). $^{13}$C{$^1$H} NMR ($C_6D_6$, 100.6 MHz, 25 °C): $\delta$ 23.8 (CH(C$H_3$)$_2$), 25.1 (CH(C$H_3$)$_2$), 26.1 ((C$H_2$CH$_2$)$_2$O) 30.4 (C$H$(CH$_3$)$_2$), 69.6 ((CH$_2$C$H_2$)$_2$O), 122.9 (*m*-Dipp), 124.4 (*m*-C$_6$H$_3$), 126.9 (*p*-Dipp), 127.1 (*m*-C$_6$H$_3$), 147.7 (*o*-C$_6$H$_3$), 150.7 (*o*-Dipp), 166.9 (*i*-C$_6$H$_3$); *i*-Dipp resonance is likely obscured by the $C_6H_6$ signal.

**Computational Methods.** Geometry optimizations on the model species, PhMMPh (M = Zn, Cd, Hg), were performed using density functional theory, where the B3LYP functional was combined with a basis set including the quasi-relativistic pseudopotentials for the metal centers and a 6-31g* basis set for C and H atoms. The CRENBL-Large orbital basis set with small core (7s6p6d valence electron space for Zn and 5s5p4d for Cd and Hg) was used for the metal centers.[24] This level of theory is hereafter described as B3LYP/ECP/6-31g*. All the geometry optimizations as well as the determination of the electronic structure for $Zn_2Ar'_2$ (**4**), $Cd_2Ar'_2$ (**5**), and $Hg_2Ar'_2$ (**6**) were performed with the Gaussian 03 package.[25]

The fragment analysis (FA) and the energy decomposition analysis (EDA) based on the method of Morokuma and the ETS partitioning scheme of Ziegler and Rauk, as implemented in ADF 2005.01 software,[26] were computed using the pure gradient-corrected BP86 functional combined with the basis set of triple-$\zeta$ quality with polarization functions (TZP) using a zero-order relativistic approximation to the energy Hamiltonian (ZORA) and non-frozen-core option (hereafter described as BP86/TZ2P/ZORA). In the EDA analysis, the instantaneous interaction energy ($\Delta E_{int}$) between the two fragments of the molecule is decomposed into three contributions: $\Delta E_P$, $\Delta E_{el}$, and $\Delta E_o$, where $\Delta E_P$ is the quantum mechanical Pauli repulsive exchange interaction between electrons possessing the same spin, $\Delta E_{el}$ is the quasi-classical attractive electrostatic interaction energy between the frozen charge distributions of the fragments, and $\Delta E_o$ is the stabilization energy corresponding to the relaxation of the Kohn−Sham orbitals to their final form. The bond dissociation energy (BDE) between the two fragments is the sum of the above instantaneous interaction energy ($\Delta E_{int}$) and a preparation energy term ($\Delta E_{prep}$), which correspond to the energy necessary to promote the two fragments from their equilibrium geometry and electronic ground state to the geometry and electronic state corresponding to the bonded compound. The bonding energy (BE) from the B3LYP/ECP/6-31g* calculations was estimated as the difference between the energy corresponding to the optimized geometry of the final compound and twice the energy of the optimized half of the molecule in the doublet spin state. Further details of the quantum mechanical calculations are included in the Supporting Information.

To compare the metal−metal bonding in **4**−**6**, we performed several theoretical studies on both molecules containing bulky Ar′ ligands and the model compounds $M_2Ph_2$. These include FA, EDA, and the estimation of the BE using the fragment-oriented approach.[27] We also compared these theoretical results with results of previously reported calculations on species exhibiting similar M−M bonding.[11,12]

**X-ray Crystallography.** Crystals of **1**−**9** were removed from a Schlenk tube under a stream of argon and immediately covered with a thin layer of hydrocarbon oil. A suitable crystal was selected, attached to a glass fiber, and quickly placed in a $N_2$ cold stream on the diffractometer.[28] The data for **1**−**6**, **8**, and **9** were recorded near 90 K on a Bruker SMART 1000 instrument (Mo K$\alpha$ radiation, $\lambda$ = 0.71073 Å, and a CCD area detector), while data for **7** were collected on a Bruker APEX instrument (Mo K$\alpha$ radiation and a CCD area detector). For compounds **1**−**4** and **6**−**9**, the SHELX version 6.1 program package was used for the structure solutions and refinements. Absorption corrections were applied using the SADABS program.[29] Crystals of **5** were determined to be twinned, and an alternative procedure (see Supporting Information) was used to "de-twin" the data and afford a solution. The structure of **5** is also disordered over two positions that are rotated 82.7° with respect to each other, such that the cadmiums appear as a "composite" atom. The resultant cadmium libration appears to bisect these two planes, and the "true" Cd−Cd distance is probably longer than the refined distance. The crystal structures were solved by direct methods and refined by full-matrix least-squares procedures. All non-H atoms were refined anisotropically. All carbon-bound H atoms were included in the refinement at calculated positions using a riding model included in the SHELXTL program. A summary of the data collection parameters for **1**−**3**, **6**, and **9** is provided in Table 1. The corresponding crystallographic details for **4**, **5**,[30] **7**, and **8** can be found in refs 13 and 14.

## Results and Discussion

**Precursor Halide Derivatives: (Ar′MI)$_{1\ or\ 2}$ (M = Zn, 1; Cd, 2; or Hg, 3).** The aryl group 12 halides **1**−**3** were used as precursors for the synthesis of the target molecular compounds Ar′MMAr′ (M = Zn, Cd, or Hg). These compounds were obtained by a simple lithium halide elimination route. Attempts

(23) Schiemenz, B.; Power, P. P. *Organometallics* **1996**, *15*, 958.
(24) Ross, R. B.; Powers, J. M.; Atashroo, T.; Ermler, W. C.; LaJohn, L. A.; Christiansen, P. A. *J. Chem. Phys.* **1990**, *93*, 6654.
(25) Frisch, M. J.; et al. *Gaussian 03*, revision B.03; Gaussian, Inc.: Pittsburgh, PA, 2003.
(26) (a) *ADF2005.01*; SCM, Theoretical Chemistry, Vrije Universiteit: Amsterdam, The Netherlands, 2005 (http://www.scm.com). (b) Morokuma, K. *J. Chem. Phys.* **1971**, *55*, 1236. (c) Kitaura, K.; Morokuma, K. *Int. J. Quantum Chem.* **1976**, *10*, 325. (d) Ziegler, T.; Rauk, A. *Theor. Chim. Acta* **1977**, *46*, 1.
(27) Rosa, A.; Ehlers, A. W.; Baerends, E. J.; Snijders, J. G.; te Velde, G. *J. Phys. Chem.* **1996**, *100*, 5690.
(28) Hope, H. *Prog. Inorg. Chem.* **1995**, *41*, 1.
(29) *SADABS*, An empirical absorption correction program, part of the SAINT-Plus NT version 5.0 package; Bruker AXS: Madison, WI, 1998.
(30) Initial work on **5** was published in ref 14. However, a slightly improved refinement was obtained, and hence we decided to resubmit the crystal data. For more details, see the Supporting Information.

***Table 1.*** Selected Crystallographic Data for **1**·$C_7H_8$, **2**, **3**, **6**·$2C_6D_6$, and **9**

| | **1**·$2C_7H_8$ | **2** | **3** | **6**·$2C_6D_6$ | **9** |
|---|---|---|---|---|---|
| formula | $C_{74}H_{90}I_2Zn_2$ | $C_{60}H_{74}I_2Cd_2$ | $C_{30}H_{37}IHg$ | $C_{72}H_{74}D_{12}Hg_2$ | $C_{60}H_{76}Cd_2$ |
| fw | 1364.04 | 1273.79 | 725.09 | 1364.73 | 1022.01 |
| habit | block | plate | plate | plate | block |
| cryst syst | monoclinic | orthorhombic | orthorhombic | orthorhombic | orthorhombic |
| space group | $P2_1/c$ | $P2_12_12_1$ | *Pnma* | *Ccca* | *Pccn* |
| *a*, Å | 13.9561(4) | 11.2906(8) | 16.7028(18) | 17.2416(9) | 20.5438(8) |
| *b*, Å | 22.5253(6) | 18.9150(12) | 20.891(2) | 25.4186(13) | 15.7065(6) |
| *c*, Å | 24.9183(6) | 26.6677(17) | 7.9572(9) | 15.1465(8) | 16.3757(6) |
| α, deg | 90 | 90 | 90 | 90 | 90 |
| *β*, deg | 121.3220(10) | 90 | 90 | 90 | 90 |
| *γ*, deg | 90 | 90 | 90 | 90 | 90 |
| *V*, Å$^3$ | 6691.8(3) | 5695.2(7) | 2776.6(5) | 6638.1(6) | 5284.0(3) |
| Z | 4 | 4 | 2 | 4 | 4 |
| cryst dimens, mm | 0.33 × 0.31 × 0.25 | 0.16 × 0.19 × 0.12 | 0.40 × 0.08 × 0.14 | 0.20 × 0.17 × 0.15 | 0.27 × 0.20 × 0.17 |
| $d_{calc}$, g·cm$^{-3}$ | 1.353 | 1.486 | 1.735 | 1.450 | 1.285 |
| $\mu$, mm$^{-1}$ | 1.679 | 1.865 | 6.670 | 4.661 | 0.840 |
| no. of reflns | 13168 | 9723 | 4176 | 4858 | 7708 |
| no. of obsd reflns | 9819 | 8272 | 3644 | 3136 | 5519 |
| *R*1, obsd reflns | 0.0323 | 0.0396 | 0.0327 | 0.0193 | 0.0486 |
| w*R*2, all | 0.1093 | 0.0855 | 0.0801 | 0.0504 | 0.1438 |

***Table 2.*** Selected Structural Data for **1**·$2C_7H_8$, **2**, and **3**

| parameter | **1**·$2C_7H_8$ | **2** | **3** |
|---|---|---|---|
| M−I (Å) | 2.6240(4)<br>2.6189(4) | 2.8114(7)<br>2.8045(7) | 2.5839(4) |
| C(ipso)−M (Å) | 1.961(3) | 2.149(6)<br>2.118(6) | 2.082(5) |
| M−I−M (deg) | 84.599(14) | 86.51(2)<br>86.64(2) | |
| C(ipso)−M−I (deg) | 133.43(9) | 135.82(17)<br>130.86(18) | 178.14(14) |
| I−M−I (deg) | 95.401(13) | 93.09(2)<br>93.66(2) | |
| C(ortho)−C(ipso)−M (deg) | 121.0(2)<br>120.5(2) | 119.4(4)<br>120.2(4) | 118.9(2) |

to use commercially available anhydrous $ZnCl_2$ instead of $ZnI_2$ did not result in good yields of a clean Ar′ZnCl product. It was found to be difficult to separate Ar′ZnCl from the LiCl byproduct because of the low solubility of Ar′ZnCl in hydrocarbon solvents. The reaction of the iodides $ZnI_2$, $CdI_2$, or $HgI_2$ with 1 equiv of LiAr′ was then employed to synthesize Ar′Zn($\mu$-I)$_2$ZnAr′ (**1**), Ar′Cd($\mu$-I)$_2$CdAr′ (**2**), and Ar′HgI (**3**), respectively. Ar′HgI (**3**) can also be obtained by the treatment of $HgI_2$ with 1 equiv of Ar′MgBr·2THF (**11**). All the aryl group 12 halides were isolated as colorless, crystalline solids. Selected structural data for **1**−**3** are provided in Table 2. The structures of **1**−**3** are presented as thermal ellipsoid plots in Figure 1.

The X-ray structure analysis showed that the arylzinc iodide **1** and arylcadmium iodide **2** formed iodide-bridged dimers in the solid state [Ar′M($\mu$-I)$_2$MAr′], whereas the arylmercury iodide, Ar′HgI (**3**), had a monomeric structure with a terminal iodine atom. A similar reaction between Li[HC(CMeNAr)$_2$] (M = Zn or Cd, Ar = 2,6-Pr$^i_2$C$_6$H$_3$) and $MI_2$ did not result in LiI elimination; instead, the lithium iodide complexes [{HC(CMeNAr)$_2$}M($\mu$-I)$_2$Li·(OEt$_2$)$_2$] were obtained.[31] In contrast, the structures of **1** and **2** showed that LiI was completely eliminated from the isolated product. Besides changes associated with the larger size of Cd vs Zn, the main difference between the structures involves the relative orientation of the Ar′ ligands. The centrosymmetric Ar′Zn($\mu$-I)$_2$ZnAr′ (**1**) has a coplanar arrangement of the central rings of the Ar′ ligands (C1−C6 and C1A−C6A), while the corresponding aryl rings in Ar′Cd($\mu$-I)$_2$CdAr′ (**2**) are oriented almost perpendicularly to each other, with a dihedral angle of 82.9° between the C1−C6 and C31−C36 planes. The Zn(1)−($\mu$-I)$_2$−Zn(1A) plane in **1** displayed a torsion angle of 37.6° relative to the central aryl rings, whereas the Cd(1)−($\mu$-I)$_2$−Cd(2) plane displayed torsion angles of 30.6° and 29.6° relative to the C1−C6 and C31−C36 planes, respectively. Like the known monodentate arylmercury halides,[32] the monomeric arylmercury iodide, Ar′HgI, **3** had a nearly linear C(ipso)−Hg−I unit, with a C(1)−Hg(1)−I(1) angle of 178.14(14)°. Geometric computational studies on the simple ionic model compounds $MX_2$ (M = Zn, Cd or Hg, X = halide) show that relativistic effects reduce the dimerization energy of the mercury dihalide by about 60−70%.[33] A similar effect is probably responsible for the monomeric structure observed for **3**.

The observed M−I distances in the arylmetal iodides varied from 2.6240(4) and 2.6189(4) Å in **1** to 2.8114(7) and 2.8045(7) Å in **2**, while a shorter M−I distance of 2.5839(4) Å was found in **3**. The large M−I bond length difference between **1**/**2** and **3** can be explained on the basis of the bridging and terminal iodine environments in each compound. Compound **2** displayed a signal at 210.9 ppm in the $^{113}$Cd NMR spectrum, which lies between the values observed for the bis(aryl)cadmium species Cd(C$_6$H$_5$)$_2$ (328.80 ppm, 1.0 M solution in *p*-dioxane) and for $CdI_2$ (55.13 ppm, 1.0 M solution in $D_2O$).[34] The mercury derivative, **3**, displayed one signal at −1293.6 ppm in the $^{199}$Hg NMR spectrum. This value is close to the −1142.6 ppm reported for Hg(CH$_3$)I (1.0 M solution in DMSO-$d_6$).[35]

**Metal−Metal Bonded Compounds: Ar′MMAr′ (M = Zn, 4; Cd, 5; or Hg, 6).** The syntheses of the dinuclear Zn$_2$Ar′$_2$ (**4**)[13] and Cd$_2$Ar′$_2$ (**5**)[14] have been previously communicated by

(31) Prust, J.; Most, K.; Müller, I.; Stasch, A.; Roesky, H. W.; Usón, I. *Eur. J. Inorg. Chem.* **2001**, 1613.

(32) (a) Pakhomov, V. I. *Kristallografiya* **1963**, *8*, 789. (b) Pakhomov, V. I. *Zh. Strukt. Khim.* **1963**, *4*, 594. (c) Tschinkl, M.; Bachman, R. E.; Gabbaï, F. P. *J. Organomet. Chem.* **1999**, *582*, 40.

(33) (a) Kaupp, M.; von Schnering, H.-G. *Inorg. Chem.* **1994**, *33*, 2555. (b) Kaupp, M.; von Schnering, H.-G. *Inorg. Chem.* **1994**, *33*, 4718. (c) Hargittai, M. *Chem. Rev.* **2000**, *100*, 2233.

(34) Cardin, A. D.; Ellis, P. D.; Odom, J. D.; Howard, J. W., Jr. *J. Am. Chem. Soc.* **1975**, *97*, 1672.

(35) Sens, M. A.; Wilson, N. K.; Ellis, P. D.; Odon, J. D. *J. Magn. Reson.* **1975**, *19*, 323.

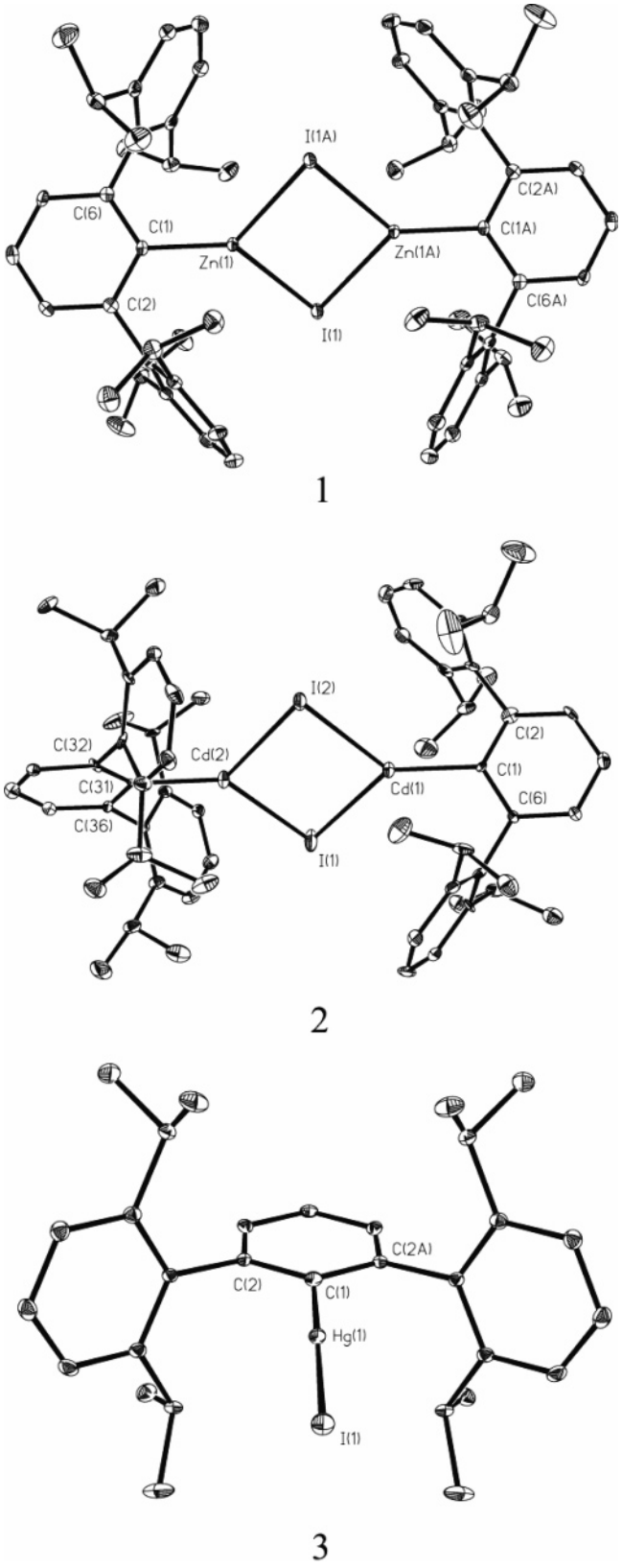


***Figure 1.*** Thermal ellipsoid (30%) plots of **1**−**3**. Hydrogen atoms are not shown for clarity.

us. Unlike **4**, which was synthesized by the simple reduction of **1** with sodium, compound **5** was prepared by the addition of 2 equiv of NaH to **2** (see below). A straightforward lithium halide elimination route was investigated for the reaction of the

***Scheme 1.*** Synthetic Routes to the M−M Bonded Dimers $M_2Ar'_2$ (M = Zn, Cd, and Hg)

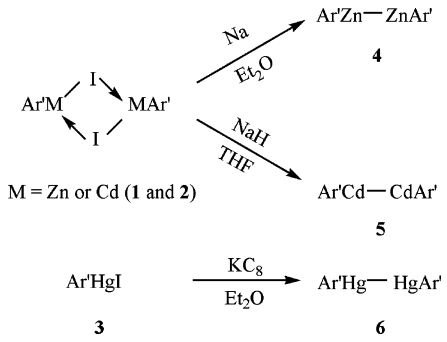


commercially available $Hg_2I_2$ salt with 2 equiv of MgAr′Br·2THF (**11**) for the synthesis of $Hg_2Ar'_2$ (**6**). However, disproportionation occurred to yield the arylmercury(II) halide **3** and metallic mercury, indicating that the ionic $[Hg_2]^{2+}$ core unit does not remain intact during its reaction with **11**. Fortunately, the dinuclear $Hg_2Ar'_2$ (**6**) could be prepared by the simple reduction of **3** with $KC_8$. The synthetic routes to the metal−metal bonded Ar′MMAr′ (M = Zn, Cd, or Hg) are summarized in Scheme 1, and the structures of **4**−**6** can be found in Figure 2. Selected structural data for **4**−**6** are provided in Table 3.

As illustrated in Figure 2, X-ray crystal crystallography confirmed the presence of a homonuclear Hg−Hg bond in **6**. The observed Hg−Hg distance of 2.5738(3) Å in **6** was *ca.* 0.30 Å shorter than the sum of Pauling's single-bond metallic radii for mercury, 2.88 Å,[36] indicating that a considerable Hg−Hg bonding interaction was present. The Hg−Hg distance in **6** is *ca.* 0.08 Å shorter than the value of 2.6569(8) Å in silylated derivative $Hg_2[Si(SiMe_2SiMe_3)_3]_2$ (**12**),[8] but it is within the bond length range of *ca.* 2.49−2.59 Å in the other related compounds, such as the ionic species $[Hg_2(Me_6C_6)_2][AlCl_4]_2$[37a] and the tetranuclear $(np_3)Co-Hg-Hg-Co(np_3)$ complex ($np_3 = N(CH_2CH_2PPh_2)_3$).[37b] The significant bond length difference between compounds **6** and **12** suggests that the ligands exert a large influence on the nature of Hg−Hg bonding interaction. The shorter Hg−Hg bond length in **6** relative to **12** and the cadmium species **5** is consistent with a stronger M−M bonding interaction and a larger HOMO−LUMO energy gap. It is also notable that the Hg−C distance (2.098(3) Å) is shorter than that of Cd−C (2.138(3) Å), consistent with the smaller size of Hg. The pale yellow color of **12** in comparison to the colorless **6** is consistent with the presence of a lower HOMO−LUMO gap and a weaker Hg−Hg bond in **12**. The greater electron-withdrawing effect of the terphenyl ligand in comparison to that of the silyl group is also seen in the $^{199}$Hg NMR spectra. Compound **12** displayed a signal at −104.5 ppm, while **6** had a more deshielded signal at 150.5 ppm. The crystal structures of **4**−**6** showed that the compounds have very similar geometries, wherein the two Ar′ ligands are arranged in a nearly orthogonal orientation to each other, providing effective steric protection of the metal−metal core. An almost linear arrangement is observed for the [C(ipso)−M−M−C(ipso)] unit, with little or no apparent bending tendency. The angles of Zn(2)−Zn(1)−C(1), Cd(1A)−Cd(1)−C(1), and Hg(1A)−Hg(1)−C(1) are 177.5(3) avg., 177.5(3)°,

(36) Pauling, L. *The Nature of the Chemical Bond*, 3rd ed.; Cornell University Press: Ithaca, NY, 1960; Chapter 7.
(37) (a) Frank, W.; Dincher, B. *Z. Naturforsch. B* **1987**, *42*, 828. (b) Ghilardi, C. A.; Midollini, S.; Moneti, S. *J. Chem. Soc., Chem. Commun.* **1981**, 865.

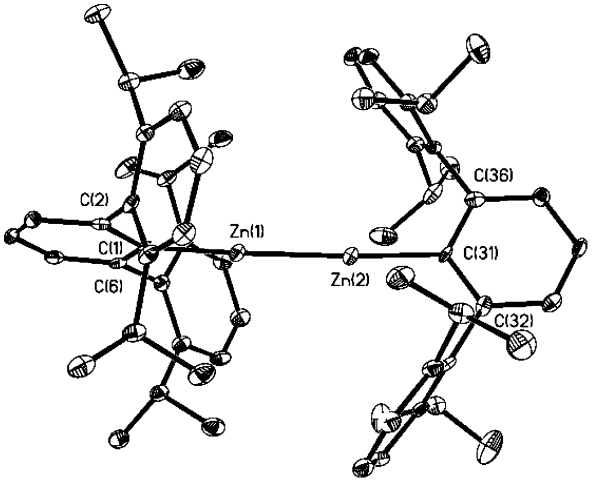


4

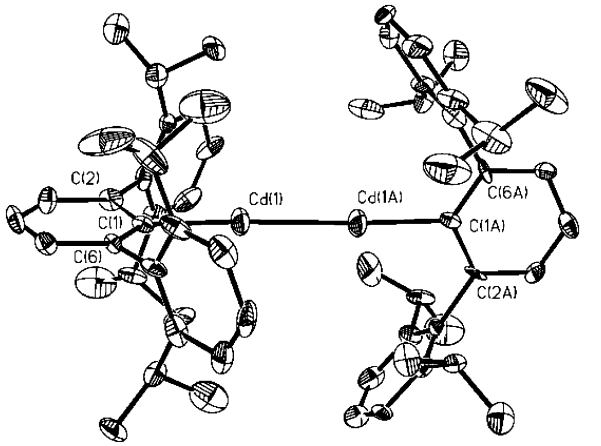


5

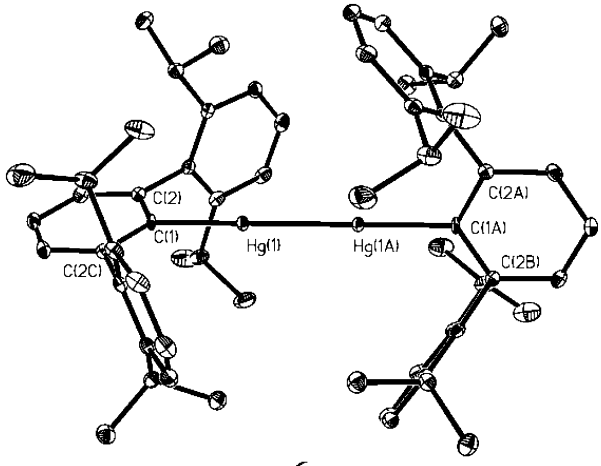


6

***Figure 2.*** Thermal ellipsoid (30%) plots of **4**−**6**. Hydrogen atoms are not shown for clarity.

and 180.0°, respectively. The M−M bonds distances varied from 2.3591(9) Å for Zn−Zn in **4** and 2.6257(5) Å for Cd−Cd in **5**, to 2.5738(3) Å for Hg−Hg in **6**. The most striking feature of the data is the shortening of *ca.* 0.05 Å in the metal−metal bond between the Cd−Cd bonded **5** and the Hg−Hg bonded **6**. This observation is consistent with the calculations on model dications $[Cd_2]^{2+}$ and $[Hg_2]^{2+}$ using the relativistic Hartree−Fock−Slater one-electron equation, which showed *ca.* 0.1 Å contraction in the M−M distance between $[Hg_2]^{2+}$ and $[Cd_2]^{2+}$ (see below for theoretical studies on model species for **4**−**6**).[15b]

***Table 3.*** Selected Structural Data for **4**, **5**, and **6**·$2C_6D_6$

| parameter | **4** | **5** | **6**·$2C_6D_6$ |
|---|---|---|---|
| M−I (Å) | 2.3591(9) | 2.6257(5) | 2.5738(3) |
| C(ipso)−M (Å) | 1.965(6) | 2.138(3) | 2.098(3) |
| | 1.974(5) | | |
| C(ipso)−M−M (deg) | 177.28(18) | 177.5(3) | 180 |
| | 177.57(18) | | |
| C(ortho)−C(ipso)−M (deg) | 120.5(4) | 116.5(6) | 120.2(3) |
| | 119.1(4) | 121.8(6) | |

**Metal Hydride Derivatives: $(Ar'MH)_{1\ or\ 2}$ (M = Zn, Cd or Hg) and Ar′Zn(μ-H)(μ-Na)ZnAr′.** Well-characterized organo group 12 hydrides are relatively rare, and there is a high tendency of these species to decompose.[18−20] Examples of structurally characterized zinc hydride compounds include $[Me_2N(CH_2)_2N(Me)ZnH]_2$,[18a] [{$\eta^3$-HB(3-$RC_3N_2H_2)_3$}ZnH] (R = $Bu^t$),[18b] $[(Me_3PN)ZnH]_4$·4THF,[18d] [{$HC(CMeNAr)_2$}Zn(μ-H)]$_2$ (Ar = 2,6-$Pr^i_2C_6H_3$),[18e] and Ar′Zn(μ-H)$_2$ZnAr′.[14] The latter two species have similar bridged structures, whereas the first three complexes have terminal hydrogen atoms. At present, only one example of an organocadmium hydride, $Tp^{t-Bu}$CdH (**13**) ($Tp^{t-Bu}$ = hydrotris(3-*tert*-butylpyrazolyl)borate),[9] has been synthesized. It was characterized by multinuclear NMR spectroscopy, but no crystal structure was obtained. There is no example of a stable, structurally characterized organomercury hydride. Studies on highly reactive organomercury hydrides suggest that these species can rapidly decompose into transient organomercury radicals.[38] The synthesis of metal hydride derivatives is also of importance to provide supporting evidence for metal−metal bonds. It is often experimentally difficult to discount the presence of a bridging hydride ligand on the basis of X-ray crystallography or spectroscopy. A further reason for our interest in metal hydrides arises from the fact that the mechanism of the Ar′Cd(μ-I)$_2$CdAr′ (**2**) reduction to $Cd_2Ar'_2$ (**4**) by NaH was not clear.[14] It was desirable to isolate a putative Ar′CdH intermediate in the reduction of **2** in order to gain insight into the reduction mechanism.

Arylmetal hydrides **7**, **9**, and **10** were each prepared by the treatment of the corresponding arylmetal halide with alkali metal hydride in THF (Scheme 2). NaH is a suitable hydride source for the synthesis of **7**[13] and **9**; however, the use of a more ionic hydride source, KH, was required to obtain **10**. As mentioned in a previous communication,[13] **7** can be further reduced by NaH to afford the unusual sodium hydride bridged species, Ar′Zn(μ-H)(μ-Na)ZnAr′ (**8**), which featured a new type of Zn−Zn bond in which the core unit,


can be viewed as a σ-antiaromatic ring.[13] It was found that the arylcadmium hydride Ar′Cd(μ-H)$_2$CdAr′ (**9**) is quite temperature sensitive, and it partially decomposes in a few hours to the Cd−Cd bonded **5** upon standing at room temperature. This observation showed that the mechanism of Ar′Cd(μ-I)$_2$CdAr′ reduction

(38) (a) Quirk, R. P.; Lea, R. E. *Tetrahedron Lett.* **1974**, *15*, 1925. (b) Hill, C. L.; Whitesidcs, G. M. *J. Am. Chem. Soc.* **1974**, *96*, 870. (c) Quirk, R. P.; Lea, R. E. *J. Am. Chem. Soc.* **1976**, *98*, 5973. (d) Russell, G. A.; Guo, D. *Tetrahedron Lett.* **1984**, *25*, 5239.

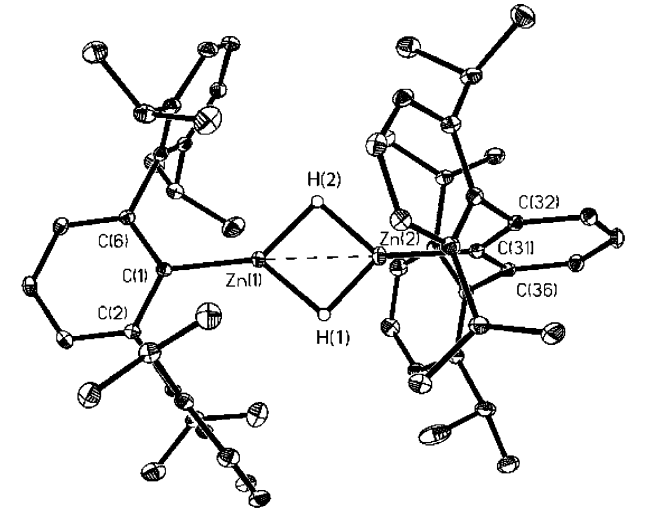


7

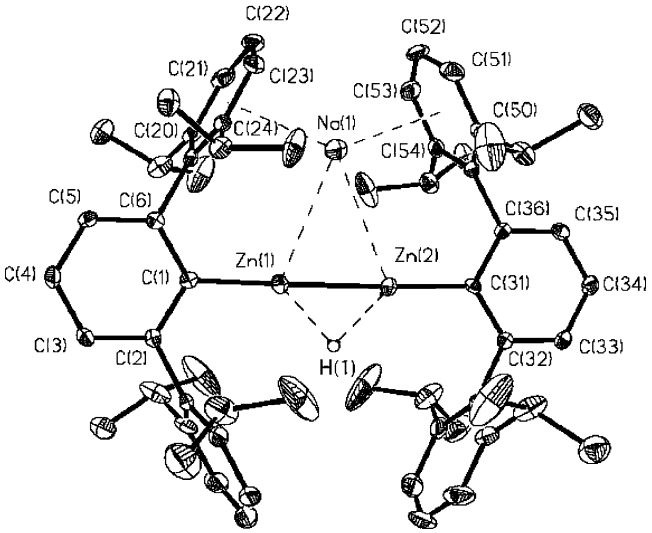


8

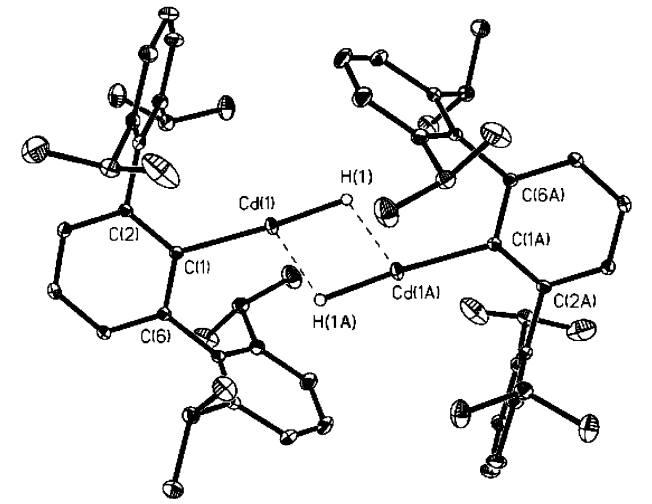


9

***Figure 3.*** Thermal ellipsoid (30%) plots of **7**−**9**. Carbon-bound hydrogen atoms are not shown for clarity.

***Scheme 2.*** Synthetic Routes to the Aryl Group 12 Hydride $(Ar'MH)_{1\ or\ 2}$ (M = Zn, Cd, or Hg) and Ar′Zn($\mu$-H)($\mu$-Na)ZnAr′

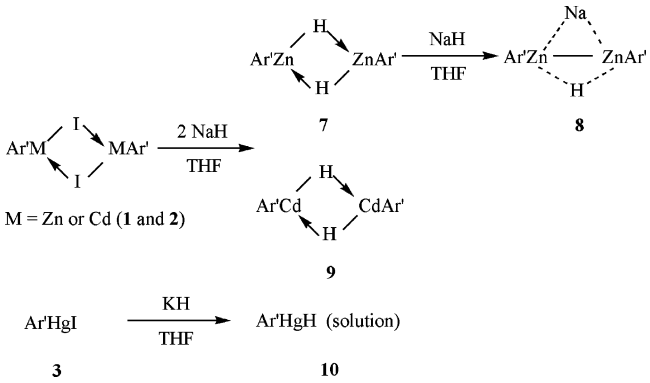


by NaH involves the initial formation of **9**, followed by the decomposition of **9** to form the more stable molecular compound **5**, with the concomitant elimination of hydrogen. Compounds **7**−**9** were obtained as colorless crystals, and their structures can be found in Figure 3. However, during the preparation of the arylmercury hydride **10**, we observed significant amounts of elemental mercury as well as the formation of Ar′H byproduct. We were unable to separate **10** from Ar′H and could not obtain a satisfactory structure for **10** in the solid state. Nevertheless, the formation of **10** as a monomer in solution was shown by $^{1}$H NMR and $^{199}$Hg NMR spectroscopy.

The arylcadmium hydride **9** has an unsymmetrically bridged structure with different Cd−H distances of 1.78(6) and 2.27(6) Å, suggesting that **9** is a loosely associated dimer. This is in contrast to the arylzinc hydride **7**,[13] where the hydrides symmetrically bridge the two zinc atoms (Zn−H distances = 1.67(2)−1.79(3) Å; H−Zn−H angles = 87.9(11)−92.0(11)°). In **9**, the terphenyl ligands are oriented in a nearly coplanar arrangement, whereas in **7** and the Cd−Cd bonded compound **5**, they are approximately orthogonal. The Cd···Cd separation of 2.9196(5) Å in **9** is *ca.* 0.3 Å longer than that in the Cd−Cd bonded species **5**, in contrast to the relatively close Zn···Zn distances in **4** and **7**, and this is also suggestive of a weak Cd−H−Cd bridging interaction.

Both arylmetal hydrides **9** and **10** were analyzed by multinuclear NMR studies. For **9**, a signal corresponding to the bridging hydride in **9** was located at 6.84 ppm in the $^{1}$H NMR spectrum in the correct intensity ratio to the aryl ligand resonances. This chemical shift is similar to that of 6.30 ppm observed in the only previously reported molecular cadmium hydride, **13**.[9] Compound **9** also displayed a $^{113}$Cd NMR chemical shift of 410.7 ppm, similar to that of **15** (348.2 ppm). However, unlike **13**, which has an observable $^{113}$Cd−$^{1}$H one-bond coupling of 2527 Hz, **9** displayed a broad signal in solution which could not be further resolved at low temperatures (−40 °C). The mercury hydride **10** displayed a signal at 14.59 ppm in the $^{1}$H NMR spectrum (Figure 4), which lies in the chemical shift range reported for alkylmercury hydrides (11.9−17.2 ppm).[20] Two symmetrically disposed satellite resonances were observed because of $^{199}$Hg−$^{1}$H coupling ($^{199}$Hg, $I = {}^{1}/_{2}$, 16.68%), and the $^{199}$Hg−$^{1}$H coupling constant was found to be 2900 Hz, which is similar to the value of 3218 Hz observed in hydridomercury (*Z*)-2-*p*-nitrophenylacrylate.[20d] In addition, the $^{1}J_{Hg-H}$ coupling constant observed in the $^{199}$Hg NMR spectrum (2910 Hz) is essentially the same as that found in the $^{1}$H NMR spectrum. The observation of a doublet in the $^{1}$H-coupled $^{199}$Hg

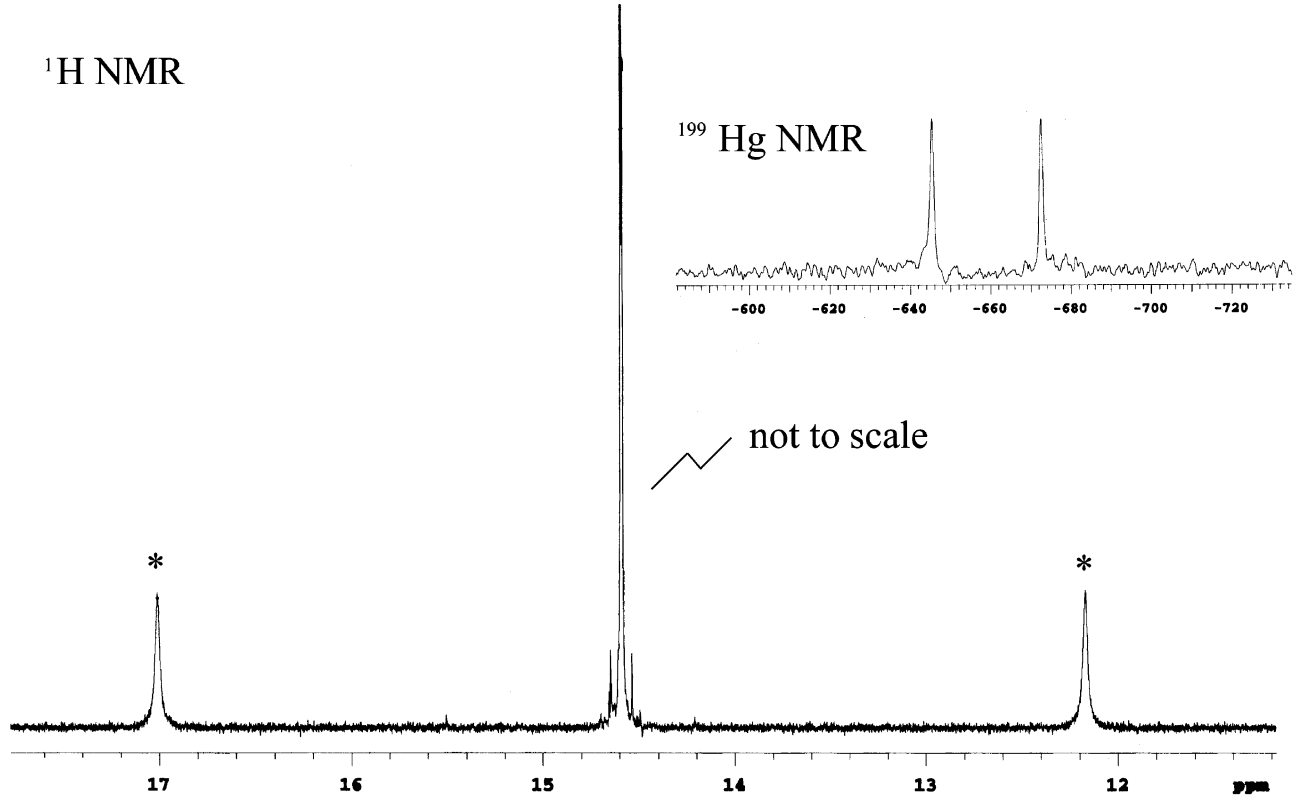


***Figure 4.*** $^1$H and $^{199}$Hg NMR spectra of **10**.

NMR spectrum is consistent with a monomeric structure for **10** in solution. It is also notable that the hydride signals progressively move to lower field, from 4.84 ppm in Ar′Zn($\mu$-H)$_2$ZnAr′ (**7**) to 6.84 ppm in Ar′Cd($\mu$-H)$_2$CdAr′ (**8**) to 14.59 ppm in Ar′HgH (**10**), as the group is descended.

**Theoretical Calculations on Group 12 Metal−Metal Bonded Compounds.** As previously reported in our original communications on $Zn_2Ar'_2$ (**4**) and $Cd_2Ar'_2$ (**5**), the HOMO is the primary metal−metal bonding orbital.[13,14] This is also true for $Hg_2Ar'_2$ (**10**) where the M−M bonding has significant contributions from metal s and $p_z$ hybrids (Figure 5). The s-orbital character of the HOMO is, in all cases, less than 50%, with the remaining contributions from $p_z$ and ligand-based orbitals. The two lowest unoccupied degenerate orbitals (LUMO and LUMO+1) are of $\pi$-symmetry, are localized on the metal−metal axis, and are derived from a combination of the empty metal $p_x$ and $p_y$ orbitals.

The extent of the p character in the metal−metal bonds of the $M_2Ph_2$ model compounds as well as in the $M_2Ar'_2$ species was investigated by fragment analysis of the various orbital contributions to the total M−M bonding. These contributions were calculated at the BP86/TZ2P/ZORA level of theory (Table 4), and this analysis clearly shows that, for all three M−M bonded $M_2Ph_2$ species, there is an important involvement of the metal $p_z$ orbitals in the HOMO. This is contrasted with the bonding situation in $Zn_2Cp^*_2$ (**14**), where the Zn−Zn bond is formed almost exclusively from 4s orbitals (99% s character at HOMO−4).[11] The Zn−Zn bond in $Zn_2Ph_2$ also has a more pronounced p character of *ca.* 30% (only metal centers were considered), as compared to that in the $Zn_2[HC(CMeNAr)_2]_2$ species (**15**) (95% s, 4% p, 1% d).[12] For the $M_2Ph_2$ series, the p character of the HOMO gradually decreases as one descends the group: 18.8% for Zn, 16.5% for Cd, and 15.8% for Hg. In addition, the heaviest congener, Hg, also has a non-negligible (5%) contribution to the HOMO from an orbital of $d_{z^2}$ parentage.

Using the fragment-oriented approach, we have computed the BEs for both the $M_2Ar'_2$ species and the $M_2Ph_2$ models at the B3LYP/ECP/6-31g* level. The calculated energies are in good agreement with previously reported theoretical data for parent congeners of the $M_2Ar'_2$ species, HMMH,[7c,10] and the two stable Zn−Zn bonded species, **14** (62.1 kcal/mol)[11] and **15** (65.2 kcal/mol) (Table 5).[12] In addition to the fragment-oriented approach, we have also performed EDA at the BP86/TZ2P/ZORA level for $M_2Ph_2$.[27] The BDE of $M_2Ph_2$ is similar to that of the M−M bonded compounds $M_2Ar'_2$ and is in agreement with the calculated BDEs of $M_2Me_2$, $M_2Cp_2$ (Cp = $\eta^5$-$C_5H_5$), and $M_2$-$Cp^*_2$ at the same level of theory.[39] The energy of the Cd−Cd bond in $Cd_2Ph_2$ was found to be 52.7 kcal/mol, *ca.* 8 kcal/mol lower than the value (60.9 kcal/mol) found in the parent Zn−Zn bonded species. The Hg−Hg bond strength in $Hg_2Ph_2$ was determined to be 54.4 kcal/mol, which lies between the energies of the Zn−Zn and the Cd−Cd bonded species. The same trend was observed for the energies computed in $M_2Ar'_2$ (56.3, 48.8, and 51.0 kcal/mol for M = Zn, Cd, and Hg, respectively). One might expect the Hg−Hg bonding energy to be the lowest of the triad because of the increase in the total Pauli repulsion, which is induced by the higher quantum number of the Hg electrons. However, the EDA of the $Hg_2Ph_2$ model clearly shows that the presence of the relativistic effects stabilizes the electrostatic and orbital terms, $\Delta E_{el}$ and $\Delta E_o$, which overcomes the increase in the total Pauli repulsion term, $\Delta E_p$, resulting in

(39) (a) Pandey, K. K. *J. Organomet. Chem.* **2007**, *692*, 1058. (b) Kan, Y. *J. Mol. Struct. (THEOCHEM)* **2007**, *805*, 127.

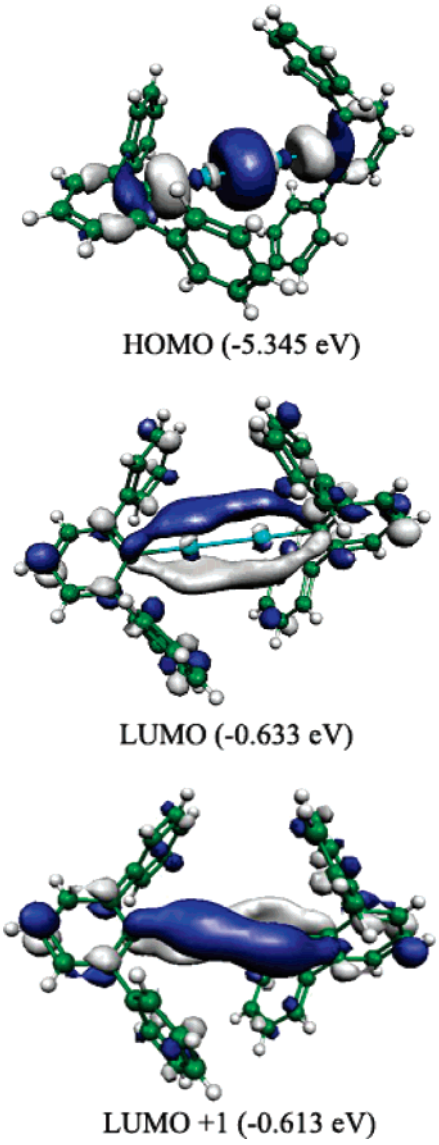


***Figure 5.*** Representation of the frontier molecular orbitals of **6**, obtained from DFT calculations (for more details, see the Supporting Information).

***Table 4.*** Contribution of Various Metal and Ligand Orbitals to the HOMO of the Model PhMMPh Species at the BP86/TZP/ZORA Level of Theory

| | % character | | | | | |
|---|---|---|---|---|---|---|
| | metal s | metal p | metal d | $C_{ipso}$ s | $C_{ipso}$ p | other[a] |
| Zn−Zn | 45.4 | 18.8 | | 3.1 | 14.1 | 18.6 |
| Cd−Cd | 47.2 | 16.5 | | 3.6 | 18.2 | 14.5 |
| Hg−Hg | 36.7 | 15.8 | 5.1 | 4.7 | 22.6 | 14.9 |

[a] Contributions from the ligand-derived orbitals in the molecule to the HOMO orbital.

***Table 5.*** Calculated M−M Bonding Energy (BE, in kcal/mol) for the $M_2Ar'_2$ and the $M_2H_2$ Species at the B3LYP/ECP/6-31g* Level of Theory Compared to Previously Reported M−M Bond Energies

| | *E*(M–M) (kcal/mol) | BSSE correction | BE[b] (kcal/mol) | BDE[c] (kcal/mol) |
|---|---|---|---|---|
| HZnZnH | −60.0 (−59.1)[a] | | | |
| PhZnZnPh | −56.6[d] | | | −60.9 |
| Ar′ZnZnAr′ | −56.3 | 0.7 | −55.6 | |
| HCdCdH | −58.6 (−55.4)[a] | | | |
| PhCdCdPh | −48.7[d] | | | −52.7 |
| Ar′CdCdAr′ | −48.8 | 0.6 | −48.2 | |
| HHgHgH | −64.1 (−61.4)[a] | | | |
| PhHgHgPh | −49.9[d] | | | −54.4 |
| Ar′HgHgAr′ | −51.0 | 0.9 | −50.1 | |

[a] Data from ref 7c. [b] Bonding energy corrected for BSSE. [c] Bond dissociation energy (BDE) of the model PhMMPh species obtained at species at the BP86/TZ2P/ZORA level of theory (details in Supporting Information). [d] Bonding energy (BE) obtained from fragment analysis at the B3LYP/ECP/6-31g* level of theory.

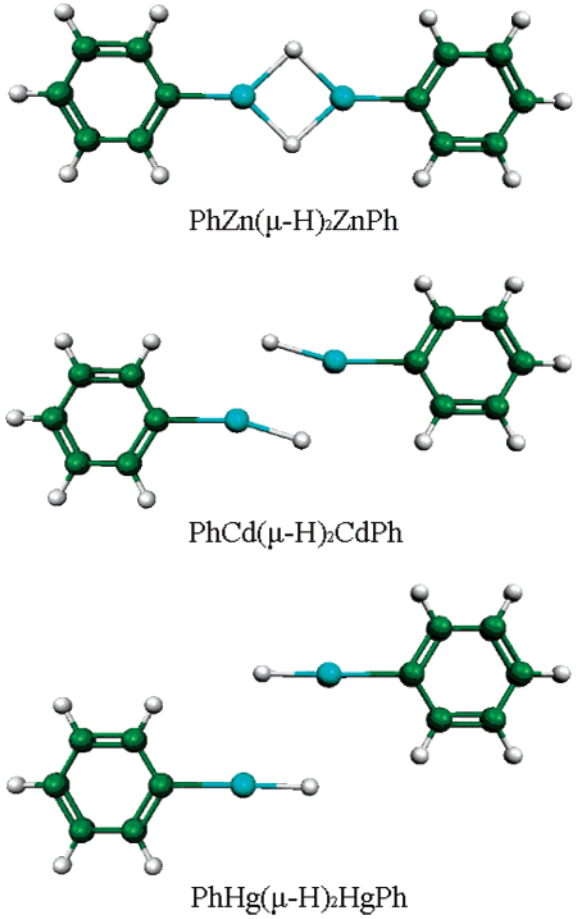


***Figure 6.*** Optimized structures of phenyl group 12 hydrides.

a higher Hg−Hg BE than that of a Cd−Cd bond. A similar BE trend within $M_2X_2$ salts (X = halogen) was also reported by Kaupp et al.[7c] and Schwerdtfeger et al.[7b]

The geometries of the $M_2Ph_2$ model species were optimized in both perpendicular ($D_{2d}$) and planar ($D_{2h}$) phenyl-to-phenyl geometries. The $D_{2d}$ perpendicular species correspond to the lowest energy form (for calculation details and structural parameters, see Supporting Information); however, the $D_{2h}$ rotational conformers lie only 0.12 (Zn), 0.21 (Cd), and 0.32 (Hg) kcal/mol higher in energy than the $D_{2d}$ minima. The calculated metal−metal bond lengths are almost identical to previously computed data for the $M_2H_2$ model species,[7c,10] yet they are slightly overestimated (max. 0.1 Å) when compared to the experimental parameters for the $M_2Ar'_2$ species obtained by the X-ray crystallography. Geometry optimizations were also performed on phenyl-substituted group 12 iodides, including three PhMI monomers and three PhM($\mu$-I)$_2$MPh dimers. All the optimized structures of the monomeric iodides exhibit linear C(ipso)−M−I bonds, and a planar phenyl-to-phenyl geometry was found for all the optimized structures of the dimers. In addition, unlike the crystal structures of **1** and **2**, where the

central M−($\mu$-I)$_2$−M plane is tilted from two central aryl rings, the iodine atoms in the optimized PhM($\mu$-I)$_2$MPh dimers are coplanar with respect to the phenyl rings. Calculations also revealed that the mercury species has the lowest dimerization energy of 4.0 kcal/mol, while for zinc and cadmium the dimerization energies are 5.3 and 9.7 kcal/mol, respectively, at the B3LYP/ECP/6-31g* level of theory. The theoretically modeled phenyl group 12 hydrides have optimized planar phenyl-to-phenyl geometries similar to those of their iodide analogues, with the hydride moieties arranged in a coplanar fashion with respect to the phenyl rings (Figure 6). However, unlike the symmetrically disposed iodine atoms in the phenyl group 12 iodides models, the optimized geometries of the corresponding cadmium and mercury hydrides have an asymmetric arrangement of the hydrogen atoms. An interesting trend in the "side displacement" of the Ph−M fragments is therefore observed in the optimized structures on going from Zn to Hg model species; the same trend was also found in corresponding arylmetal hydride species Ar′Zn($\mu$-H)$_2$ZnAr′ (**7**) and Ar′Cd($\mu$-H)$_2$CdAr′ (**9**).

## Conclusion

The first synthesis and structural characterization of the homologous M−M bonded series Ar′MMAr′ (M = Zn, Cd, or Hg; Ar′ = C$_6$H$_3$-2,6-(C$_6$H$_3$-2,6-Pr$^i_2$)$_2$) have been described. These compounds possess almost linear C−M−M−C core structures with two-coordinate metals. The M−M bond distances varied from 2.3591(9) Å for Zn−Zn to 2.6257(5) Å for Cd−Cd and 2.5738(3) Å for Hg−Hg. DFT calculations showed that the M−M bonds have significant p character in the M−M $\sigma$-bonding HOMO, and a systematic loss of p character in the bonds was calculated as one descends the group. The bond energies for both the M$_2$Ar′$_2$ species and M$_2$Ph$_2$ models were calculated using a fragment-oriented approach. It estimates a Cd−Cd bond strength of 48.2 kcal/mol, which is *ca.* 7 kcal/mol lower than the value of 55.6 kcal/mol for the parent Zn−Zn species, while the calculated Hg−Hg bond enthalpy (50.1 kcal/mol) lies between those of the Zn−Zn and the Cd−Cd bonded species at the B3LYP/ECP/6-31g* level of theory. The related arylmetal halide, Ar′MI, and the very reactive hydride, Ar′MH, precursors were also synthesized and fully characterized by X-ray crystallography and multinuclear NMR spectroscopy. The synthesis of Ar′CdCdAr′ via reduction of (Ar′CdI)$_2$ with NaH proceeds through the weakly associated (Ar′CdH)$_2$ dimer, which decomposes to Ar′CdCdAr′. The metal−metal separations observed in the dimer zinc and cadmium hydrides are significantly larger than those in the metal−metal bonded dimers.

**Acknowledgment.** We thank the National Science Foundation and the U.S. Department of Energy Hydrogen Storage Center of Excellence for financial support. R.C.F. thanks the Max Kade foundation for a postdoctoral fellowship. E.R. thanks NSERC of Canada for a postdoctoral fellowship. R.W. thanks the Alexander von Humboldt Foundation for a Feodor Lynen Research Fellowship.

**Note Added in Proof.** The synthesis and characterization of a further Zn−Zn bonded species [{Na(THF)$_2$}$_2${MeCN-(C$_6$H$_3$-2,6-Pr$^i_2$)}$_2$Zn$_2$] (Zn−Zn = 2.3994(6) Å) has been published recently: Yang, X-J.; Yu, J.; Liu, Y.; Xie, H. F.; Schaefer, H. F.; Liang, Y.; Wu, B. *Chem. Commun.* **2007**, 2363.

**Supporting Information Available:** X-ray data for **1**, **2**, **3**, **5**, **6**, and **9** (CIF); complete ref 25; details of the refinement of **5**; selected Kohn−Sham orbital surfaces of **6**; optimized structures of the PhMMPh (M = Zn, Cd, or Hg) model species at the B3LYP/ECP/6-31g* level; calculation details of the M−M bonding energy decomposition for the model PhMMPh species obtained at the BP86/TZP/ZORA level of theory; structural parameters obtained from geometry optimizations of the PhMMPh, (PhMI)$_{1\text{ or }2}$ and PhM($\mu$-H)$_2$MPh model species at the B3LYP/ECP/6-31g* level. This material is available free of charge via the Internet at http://pubs.acs.org.

JA072682X